Journal of Applied Pharmaceutical Science Vol. 14(04), pp 143-154, April, 2024
Available online at http://www.japsonline.com
DOI: 10.7324/JAPS.2024.158020
ISSN 2231-3354

Design and assessment of *in silico* screened diosmin incorporated ultra-flexible topical lipid gel system for the treatment of varicose vein

Akhilesh Dubey[1], Amitha Shetty[1], Chaithra R. Shetty[2], Namdev Dhas[3], Anup Naha[3], Pratika Bhandary[1], Srinivas Hebbar[3*]

[1]Department of Pharmaceutics, NGSM Institute of Pharmaceutical Sciences, NITTE (Deemed to be University), Mangaluru, India.
[2]Department of Pharma Chemistry, NGSM Institute of Pharmaceutical Sciences, NITTE (Deemed to be University), Mangaluru, India.
[3]Department of Pharmaceutics, Manipal College of Pharmaceutical Sciences, Manipal Academy of Higher Education, Manipal, India.

ARTICLE HISTORY

Received on: 19/12/2023
Accepted on: 01/03/2024
Available Online: 05/04/2024

Key words:
Diosmin, ultra-flexible lipid nano gel, carbopol, varicose veins.

ABSTRACT

The ultra-flexible lipid gel system (UFLGS) consists of bilayer lipid membranes, responsible for highly elastic and deformable vesicles compared to conventional topical systems. Varicose veins are abnormal, dilated blood vessels resulting from weakening in the wall of the blood vessels. A flavonoid diosmin is highly potential to alleviate circulatory issues by altering blood veins' elasticity and suppleness. Schrodinger 2023-1 suite device was used for molecular docking study. Ultra-flexible lipid nanosuspension (UFLNS) was developed and optimized. Then, they are characterized for Fourier transform infrared spectroscopy, differential scanning calorimetry, entrapment efficiency, transmission electron microscopy, atomic force microscopy, and turbidity measurement studies. After incorporating into the aqueous gelling agent Carbopol 934, Diosmin UFLGS (DUFLGS) was compared with the diosmin conventional gel system (DCGS) for its physicochemical properties. The docking score was –8.507, representing good interaction and binding affinity for nuclear factor-kappaB inducing kinase. The particle size, polydispersity index, and surface charge of optimized diosmin-loaded UFLNS (DUFLNS) were found to be ideal values 144.56 ± 5.1 nm, 0.397 ± 0.13, and –24 ± 0.9 mV, respectively. The results of DUFLNS, DUFLGS, and DCGS showed skin retention values of 55.5% ± 13%, 83.44% ± 12%, and 66.39% ± 14%, respectively. The sustained release of the DUFLGS is owing to the elasticity of the ultra-flexible lipids, thereby the penetration enhanced compared to DCGS.

INTRODUCTION

The aberrant, dilated, and convoluted veins in the leg are called varicose veins which are observed in 10%–30% of the general population [1]. The condition is caused by the improper working of the valves within the veins and reduced elasticity of the veins that allows the deoxygenated blood to flow backward and accumulate in the superficial veins. It increases hydrostatic pressure, triggers leucocytes to adhere to capillary endothelium, and initiates an inflammatory response. As a result, the fluid that produces edema becomes permeable to the capillaries [2]. The patients associated with varicose veins show aching, heaviness, itching, skin changes, ulcers, bleeding, phlebitis, throbbing, fatigue, pruritus, ankle swelling, and tenderness [3]. The usage of herbal products or phytoconstituents has been an emerging trend in treating various diseases due to its fewer adverse effects, lower therapy costs, and more reliable action [4]. Diosmin (diosmetin 7-O-rutinoside, $C_{28}H_{32}O_{15}$MW) is a natural flavonoid, found mostly in the pericarp of citrus fruits belonging to the Rutaceae family. It has a variety of biological effects, including being an anti-inflammatory, antioxidant, antidiabetic, and antitumoral agent [5]. The diosmin is an excellent therapeutic moiety commonly used in treating chronic venous insufficiency, lymphedema, and varicose veins for its phlebotonic and vascular-protective function. The medicinal properties of diosmin are related to its ability to prevent noradrenaline from being absorbed and metabolized either by the veins wall. This leads to a rise in vascular tone

*Corresponding Author
Srinivas Hebbar, Department of Pharmaceutics, Manipal College of Pharmaceutical Sciences, Manipal Academy of Higher Education, Manipal, India. E-mail: hebbar.srinivas @ manipal.edu

with beneficial effects and, hence, decreases the elasticity and permeability of veins [6]. The drug exhibits anti-inflammatory actions by suppressing the production of proinflammatory cytokines by limiting the activation of nuclear factor-kappaB (NF-κB) pathways and decreasing T-cell receptors [7]. Recent research approaches employ *in-silico* molecular docking studies as a key technique to identify the primary target, which offers information on the site-specific functions of the drug and receptor channels.

The oral administration of diosmin rapidly hydrolyses in the intestinal flora due to poor miscibility with the lipids and absorption as an aglycone derivative diosmetin. The poor absorption of the phytoconstituents directly relates to reducing its bioavailability. Hence, generally larger dose is required in the oral treatment, which is not a patient-benefit approach. Therefore, adopting a novel drug delivery system via topical drug distribution through the skin layer is the most suitable approach to a specific site with controlled and sustained drug delivery to improve therapeutic efficacy. The ultra-flexible topical lipid carrier systems have been characterized for a topical application, consisting of internal aqueous partition surrounded by lipid vesicles; morphologically like liposomes, operationally similar to transferosomes, appropriately deform to move through skin pores far lesser than their size [8]. It can also work as a penetration enhancer, disrupting the stratum corneum's tightly structured intercellular lipids and allowing drug molecules to penetrate into and through the stratum corneum [9]. The interaction of the polar substituent of soy phosphatidylcholine with the hydrophilic head of diosmin will increase solubility in the ultra-flexible technique.

Therefore, the study's objective was to formulate diosmin-loaded ultra-flexible lipid nanosuspension (DUFLNS) incorporated into carbapol gel called a diosmin UFLGS (DUFLGS) and evaluate its *in vitro* characterizing parameters.

MATERIALS AND METHODS

Materials

Diosmin, (95%) Yucca Enterprises, Mumbai. Soya phosphotidyl choline, Himedia Lab Pvt. Ltd., Mumbai, Cholesterol Loba Chemie Pvt. Ltd., Mumbai, Tween 80 Loba Chemie Pvt. Ltd., Mumbai, Diethyl ether Merck Ltd., Mumbai Carbopol 934 Loba Chemie Pvt. Ltd., Mumbai, Triethanolamine Nice Chemicals Pvt. Ltd., Kerala. Sodium deoxycholate, dimethyl sulfoxide (DMSO), isopropyl alcohol, and all additional chemicals were of analytical reagent grade with no further purifications.

Molecular docking studies

The crystal structures of NF-κB inducing kinase (NIK) (PDB ID: 4G3D) from the Research Collaboratory for Structural Bioinformatics Protein Data Bank were used for molecular docking studies as the NF-κB transcription factors are critical mediators of inflammatory and immune responses [10]. 4G3D is a crystal structure of murine NIK with a resolution of 2.90 Å. Maestro 13.5.128, Schrodinger 2023-1 device was used for molecular docking study [11]**.** Both the ligand and selected target protein were prepared initially using the ligprep and protein preparation wizard applications, respectively. Grid box was created by generating receptor grids. In the end, extra precision molecular docking was performed.

Preparation of DUFLNS

A lipid mixture was created by dissolving soya lecithin and cholesterol in a 3:1 ratio in separate organic solvents, diethyl ether, and chloroform, respectively. Tween 80 (0.2% w/v) was incorporated into the lipid mixture and dissolved, forming a uniform solution. The homogeneous solution was then allowed to stand at room temperature for 24 hours, enabling the gradual evaporation of organic solvents and forming a thin lipid film. Subsequently, a solution of diosmin (10 mg/ml) in DMSO was gently poured onto the thin lipid film. The final volume of nanosuspension was 5 ml. Sodium deoxycholate (2% w/v) as an edge activator was introduced to the transfersomes in phosphate buffer solution (PBS) (pH 7.4). To enhance diosmin encapsulation within the transfersomes, the diosmin-loaded lipid film was subjected to sonication using a probe sonicator (FS-600, Frontline Electronics and Machinery Pvt. Ltd., India) operating at a frequency of 20 KHz for 2 minutes [12,13].

Design of experiments (DoE)

The impact of various input parameters on the preparation of UFLNS was assessed using the DoE method [14]. The design consists of a concentration of independent variable factors such as soya lecithin, cholesterol, Tween 80, and sodium deoxycholate. These elements influence vesicle formation and rigidity of the vesicle, which provides flexibility and deformability, correspondingly. The experimental conditions were optimized according to the software Design-Expert® runs (Version 10.0.1; Stat-Ease). A central composite design and response surface methodology (RSM) were used to operate at two levels generating 25 runs. The goal responses of dependable variables are particle size (PS) (nm), polydispersity index (PDI) to minimize, and Zeta potential (ZP) (mV) to maximize. The relevant components and the levels (–1 and +1) were created for the experiment and the level of variables was depicted in Table 1.

Characterization of optimized DUFLNS

Study of morphological properties of vesicles

The developed formulations were visually inspected under the high-power optical microscope for the vesicles' morphological characteristics, such as shape and appearance. The diluted suspension was observed under microscopic magnification of a 15 × 45x lens connected to the particular software "BIOVIS," and the photomicrographs were recorded [12].

Study of PS, PDI, and ZP

The Malvern zeta sizer instrument (Malvern Zetasizer UK based-Zen 3600) was used to find the mean DUFLNS ZP, PDI, and PS. The mean diameter is determined by utilizing the spectrophotometric method, while the range of the size distribution is determined by PDI. The ZP also displays the

Table 1. Factors and their corresponding levels used for independent variables.

Factor	Independent variables	Level (–1)	Level (+1)
A	Soya lecithin (µmol)	150	300
B	Cholesterol (µmol)	25	100
C	Tween 80 (µmol)	5	10
D	Sodium deoxycholate (µmol)	25	100

dispersion systems' stability by reflecting the shift in electrical charges at the vesicle's surface [15].

Entrapment efficiency (EE) and drug loading capacity (DL)

The amount of free drugs that are entrapped in the suspension using the centrifugation process was calculated to estimate the EE of the DUFLNS [16]. At first, 5 ml of DUFLNS was poured into a centrifugation tube and centrifuged by using a cooling centrifuge (Remi Electrotechlink Ltd., Mumbai) at 10,000 rpm at 4°C for 10 minutes [17]. Later, 1 ml of supernatant was diluted using 9 ml of PBS, absorbance near 268 nm was assessed using spectrophotometry to estimate the concentration of unentrapped drug [18].

The equation below was utilized to calculate the percentage of EE:

$$\% \text{ EE} = \frac{\text{Total drug added} - \text{Unentrapped drug in supernatant}}{\text{Total drug added}} \times 100$$

$$\% \text{ DL} = \frac{\text{Total drug added} - \text{Unentrapped drug in supernatant}}{\text{Total drug added} + \text{Total amount of lipids added}} \times 100.$$

Fourier transform infrared spectroscopy (FTIR)

FTIR is a valuable tool for investigating molecular interactions within a formulation. This analytical technique enables researchers to assess the chemical compatibility between a drug substance and excipients, thereby ensuring the stability and efficacy of the formulation. During FTIR analysis, a small amount of the sample is placed on a crystal diamond and recorded using specialized software. IR spectra of soya lecithin, cholesterol, sodium deoxycholate, diosmin, physical mixture, and DUFLNS were analyzed at room temperature using Bruker FTIR spectrophotometer, equipped with liquid nitrogen-cooled mercury cadmium telluride detector at a nominal resolution of 2 cm^{-1}. The wavenumber of a physical mixture's characteristics peak was compared to that of a pure sample, and the results were interpreted [19,20].

Differential scanning calorimetry (DSC)

Shimadzu differential scanning calorimeter (DSC-50, Kyoto, Japan) was used to examine the DSC thermograms of soy lecithin, cholesterol, sodium deoxycholate, diosmin, and DUFLNS. 99.9% pure indium was used for the equipment validation. To produce the DSC thermograms, 3–4 mg of samples were put in an aluminum pan with a flat bottom and heated at a continuous scanning rate of 10°C/minute between 20°C and 400°C while being exposed to nitrogen gas [21].

Surface morphology study

Transmission electron microscopy (TEM)

In this study, we employed TEM to accurately determine the shape and morphology of DUFLNS vesicles. To prepare the samples, a diluted optimized DUFLNS solution of 2 µl was carefully deposited onto carbon-coated copper grids with a mesh size of 400. The sample was then subjected to a drying period of 5–10 minutes using an infrared lamp. This crucial step ensured the removal of excess liquid and facilitated the firm adhesion of the sample to the grid. To enhance the visibility of the DUFLNS vesicles, we applied negative staining to the sample on the grid. This specialized staining process significantly improved contrast, enabling us to obtain clearer images of the DUFLNS vesicles during TEM analysis [22]. Utilizing the CM 120 Bio Twin TEM from Philips Electron Optics BV, Netherlands, we meticulously examined the surface morphology and vesicle shape, including characteristics such as roughness, smoothness, and aggregation. The precise imaging and analysis allowed us to gain valuable insights into the structural features of the DUFLNS vesicles, contributing to a comprehensive understanding of their properties and potential applications.

Atomic force microscopy (AFM)

In this study, we utilized an AFM to conduct a comprehensive analysis of the DUFLNS's surface morphology in three dimensions (3-D). The AFM instrument used for this purpose was the Innova SPM atomic force microscope, provided by Bruker, Santa Barbara, CA. To begin the analysis, a thin smear of the DUFLNS sample was carefully deposited onto a Mica Disc. Subsequently, the sample was visualized in contact mode using specialized AFM tips. The scan was performed at a speed of 1.2 Hz, and the resonance frequency was set to 267–328 kHz. In contact mode, the AFM tip was in direct contact with the sample during scanning. The topography of the DUFLNS sample induced a vertical deflection of the cantilever as the AFM tip scanned along the surface. To measure this deflection accurately, a fiber optical interferometer was employed. This interferometer helped obtain high-resolution images for height and diameter measurements, as well as topographical 3-D and phase-contrast images. By leveraging the capabilities of the Innova SPM atomic force microscope, we were able to gain detailed insights into the three-dimensional surface morphology of DUFLNS [23].

Turbidity measurement

The amount of surfactant present or its influence on the formulation is proportional to the turbidity. If the formulation is turbid, there may be a chance of more drug leakage from the vesicles. The turbidity of the DUFLNS was determined by the Systronics Nephelometer (Systronics Nephelometer, Gujarat). The nephelometer calculates the amount of light that scatters found to be proportional to the quantity of particles within sample [24].

Preparation of DUFLGS and diosmin conventional gel system (DCGS)

A determined quantity of carbopol 934 was mixed with 100 ml of water and then aggressively agitated over 2 hour. After that, allowed hydrating for 24 hours. pH 6.8 was adjusted by the addition of triethanolamine. The 1%, 1.5%, and 2% w/v carbopol gel concentrations were prepared and evaluated for viscosity, spreadability, and consistency. Based on parameters, 1.5% w/v was found to be the optimized concentration. The DUFLNS and drug suspension were incorporated separately into the gel base, and the pH and consistency of the gel were maintained [25].

Evaluation of DUFLGS and DCGS

Determination of pH

The gel formulation's pH should be close to that of the skin for penetration and drug absorption. The electronic pH meter's sensor is mounted on the gel surface, and it was given a minute to acclimate. Using the pH buffer solution, the pH meter was calibrated. The pH of both the gels was determined in triplicate. The skin pH of topical gel formulation should be within the range of 4–6 [26].

Viscosity measurement

A fluid's viscosity is an indication of its flow resistance. Using a digitized Brookfield viscometer (DV-11 +pro) fitted with T-bar spindle No. F96, the viscosity of the DUFLGS and DCGS was assessed at various speed ranges of 5, 10, 20, 50, and 100 rpm [27].

Spreadability test

The word spreadability refers to the area of the region across which the gel spreads upon application on the skin's surface. A customized device made out of glass panes slides was used to assess the spreadability of the gels. Between the two slides, 0.5 g of each gel was positioned over a 5 cm length. The uppermost slide was loaded with 100 g of weight for 5 minutes and removed. The slide's edge had some extra gel on it, which was scraped out. The lower slide was then tied to the hook, while the top slide was connected to the string movements connected to this pan via a simple pulley. The amount of time that passed after a 30 g load was applied to the pan to separate the top slide from the descending slide was measured. The spreadability was then determined using the following formula:

$$\text{Spreadability} = \frac{m \times l}{t}$$

where m is the weight affixed to the top slide (30 g), l means the glass slide's length (5 cm), and t indicates the amount of time, in seconds. The spread ability in terms of unit second increases with the amount of time needed to separate the two slides [28].

Drug content

Separately, 50 ml of stock solution of phosphate buffer (pH 7.4) was used to dissolve 1 g of the DUFLGS and DCGS, each of which is equal to 10 mg of diosmin. Then, the sample was diluted before being tested for absorbance with a UV spectrophotometer at 268 nm [29].

Degree of deformability

The deformability nature of ultra-flexible vesicles is proportional to their penetration capability through a permeability barrier. DUFLGS and DCGS were forcibly extruded through a polycarbonate filter with a 2 ml volume and 50 nm pore size held in metal holders with 2.5 bar pressure. The proportion of vesicle dispersion discharged every minute for 10 minutes was measured. The formula shown below was employed to calculate the vesicle membrane deformability [30,31].

$$D = J \times (\text{rv}/\text{rp})^2$$

where D = deformability of the vesicle membrane, J = flux that was discharged over a 10 minute period, rv = vesicular size (after passes), and rp = pore size of the barrier (100 nm).

Ex vivo permeation and deposition study

An *in vitro* skin permeation investigation was undertaken to investigate whether drugs may pass through the goat skin membrane. The goat abdominal skin membrane was selected for the study since its morphology is similar to the human skin epithelium. A modified Franz diffusion cell was used for an *in vitro* permeation investigation [32]. The fresh goat abdominal skin was collected from the slaughterhouse, and the outer skin was removed and hydrated in phosphate buffer pH 7.4. The receiver chamber was loaded with phosphate buffer pH 7.4 at 37°C ± 0.5°C. The tissue was then placed on the receptor compartment diagonally. 1 ml of DUFLNS, 1 g each of DUFLGS and DCGS was loaded over the skin membrane separately and agitated with the magnetic stirrer at a rate of 50 rpm. The sample of 1 ml each is withdrawn from the receptor section and replaced with an equal quantity of phosphate buffer at pH 7.4 is required to keep the sink state at a prescribed time. The 12 hours were allocated to the investigation to measure the absorbance and a UV spectrophotometer was used at 268 nm. After the permeation study, the diffusion cell's skin was removed, and it was thoroughly cleaned with ethanol: phosphate buffer pH 7.4 (1:1), and water to eliminate the excess drug. The tissue was detached, homogenized in ethanol: phosphate buffer (1:1), and left at room temperature until 6 hours without any disturbance. After that, it was centrifugation at 5,000 rpm for 5 minutes to determine the diosmin content using a UV spectrophotometer [33].

Investigation of drug release-in vitro

A modified Franz diffusion cell was used in an *in vitro* drug release investigation to ascertain the extent and duration of drug release integrated into the DUFLNS, DUFLGS, and DCGS. In 7.4 pH phosphate buffer, a dialysis membrane was preserved for 24 hours before use. The receptor compartment was kept at a temperature of 37°C with a 7.4 pH phosphate buffer solution. Between the donor and receiver sections, the dialysis membrane was attached, and 1 ml of optimized DUFLNS and 1 g each of DUFLGS and DCGS were placed over the dialysis membrane employing a magnetic stirrer and stirring at a rate of 50 rpm. At predetermined intervals, 1 ml from each sample

was taken from the sample cell while maintaining the sink state. Samples are taken at multiple time points, such as 0.5, 1, 2, 4, 6, 8, and 12 hours to capture the drug release behavior adequately. The absorbance at 268 nm was measured during the study's 12-hour duration [34]. To understand the mechanism of drug release, a kinetic study was carried out by using selected models. The R^2 and K values obtained from the various models were used to select the model that suited the data the best. Diffusion exponent was also used in mathematical models to describe the rate at which a vesicles spreads or diffuses through a medium. It is commonly used in the context of Fick's law of diffusion, which describes the diffusion of a substance from an area of high concentration to an area of low concentration [35].

Statistical analysis

Each evaluation parameter was carried out in triplicates. The statistical evaluations were performed using correlation coefficients (R^2) with suitable standard deviations.

RESULTS

Molecular docking studies

When diosmin was docked against the crystal structure of human NIK the score was –8.507. There are four hydrogen bond interactions were observed between LEU471, ASP519, ARG408, and GLY407 with different phenolic and alcoholic –OH groups of diosmin. A metal coordination was seen between phenolic –OH and Mg^{2+} ion as shown in Figure 1. NF-κB is activated by extracellular stimuli including proinflammatory cytokines, mitogens, DNA-damaging agents, and microbial agents. Based on the docking score, diosmin is believed to show good interaction and binding affinity for NIK. Hence, the drug was considered to be an effective therapeutic moiety in the treatment of varicose veins.

Design of experiments

DUFLNS prepared as per the requirements provided by the Design-Expert® software (Version 11.0.3.0 64-bit, Stat-Ease Inc. Minneapolis, MN) using central composite designs, and accordingly, 25 batches were prepared based on different concentrations of lipids and surfactants (Table 2). The PS (120.35–340.16 nm), PDI (0.286–0.926), and ZP (–12.8 to –32.7 mV) measurement showed significant variations in all the trials. (Fig. 2a–c) Equations (1)–(3) show the central composite design model generated after completing ANOVA analysis for the most significant factors as well as interactions in each of the three responses. The positive mark shows a linear relationship between the response and the factor, whereas the negative sign shows an inverse relationship.

$$PS = +184.71 + 31.19*A + 17.68*B + 10.05*C + 8.31*D \quad (1)$$

$$PDI = +0.5420 + 0.1072*A + 0.0576*B + 0.0300*C + 0.0340*D \quad (2)$$

$$ZP = –23.10 – 1.85*A – 0.9308*B – 3.00*C + 0.2708*D \quad (3)$$

A, B, C, and D stand for the coded values for soya lecithin, cholesterol, Tween 80, and sodium deoxycholate, correspondingly.

Optimization

The model generated for PS was significant as its F value was 2.95 and that had a p-value of less than 0.05. The value separated by adjusted (R^2 0.2457) and the predicted (R^2 0.0234) model R-squared value was <0.2 indicating reasonable agreement between the two. As shown in Equation (1), there was a major effect of the amount of soya lecithin and cholesterol on the PS. It was determined that the model created for the PDI was relevant as it had a p-value of <0.05 and the F-value was found to be 2.87. The adjusted (R^2 0.2379) and predicted (R^2 0.0207) model R-squared values were found to differ by less than 0.2, demonstrating that there is some degree of agreement between the two. The size distribution was significantly impacted by the soy lecithin and cholesterol content of the ultra-flexible liposomes, as shown in Equation (2). The model generated for the ZP was found to be significant as it had a p-value of <0.05 and an F value of 3.43. The variation seen between the adjusted (R^2 0.2964) and the predicted (R^2 0.0727) model R-squared value was found to be less than 0.2, suggesting a fair understanding between the two. The amount of soya lecithin and cholesterol had a major effect on the ZP as shown in Equation (3). The ZP of the optimized DUFLNS was confirmed to be –24 mV, and the PS was 144.56 nm with a size distribution (PDI) of 0.397. The percentage deviation range between observed and expected was determined and shown in Table 3.

Characterization of optimized DUFLNS

Morphology, average PS, ZP, and PDI

The optimized DUFLNS was found to be a milky suspension due to refraction and reflection of light without any phase separation. The PS of the DUFLNS was observed using a Malvern Zeta sizer depending on the fundamentals of the

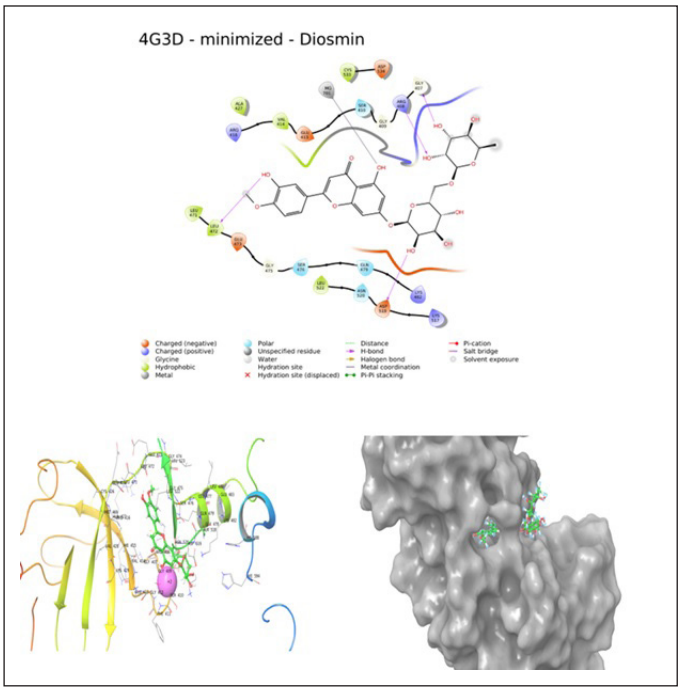

Figure 1. Docking study of diosmin.

Table 2. Experimental design and the observed response.

Std	Run	Factor 1 A: Soya Lecithin	Factor 2 B: Cholesterol	Factor 3 C: Tween 80	Factor 4 D: Sodium deoxycholate	Response 1 PS	Response 2 PDI	Response 3 ZP
		µmol	µmol	µmol	µmol	nm		mV
11	1	–1	1	–1	1	155.37	0.482	–12.2
23	2	0	0	0	–2	124.55	0.321	–25.88
22	3	0	0	2	0	135.22	0.372	–26.8
1	4	–1	–1	–1	–1	160.89	0.399	–16
4	5	1	1	–1	–1	217.28	0.795	–15.8
7	6	–1	1	1	–1	153.44	0.426	–26.5
5	7	–1	–1	1	–1	165.35	0.452	–23.7
12	8	1	1	–1	1	312.75	0.916	–20.7
9	9	–1	–1	–1	1	163.72	0.423	–14.6
16	10	1	1	1	1	340.16	0.987	–30.5
6	11	1	–1	1	–1	180.71	0.663	–24.5
10	12	1	–1	–1	1	167.37	0.666	–20.1
25	13	0	0	0	0	120.35	0.286	–25.66
20	14	0	2	0	0	165.83	0.411	–24.98
2	15	1	–1	–1	–1	207.19	0.576	–18.7
15	16	–1	1	1	1	186.48	0.739	–27.3
24	17	0	0	0	2	130.32	0.331	–26.13
17	18	–2	0	0	0	142.79	0.408	–24.75
8	19	1	1	1	–1	320.36	0.926	–32.7
18	20	2	0	0	0	170.38	0.412	–25.5
13	21	–1	–1	1	1	167.27	0.431	–12.6
19	22	0	–2	0	0	140.26	0.356	–25.11
21	23	0	0	–2	0	129.29	0.389	–27.1
3	24	–1	1	–1	–1	180.23	0.498	–18.4
14	25	1	–1	1	1	280.29	0.886	–31.3

technique of dynamic light scattering. The PS and PDI were found to be 144.56 ± 5.21 nm and 0.397 ± 0.13 signifies narrow range vesicle size distribution whereas ZP was observed to be –24.5 ± 0.95 mV indicating reasonable repulsive force and better stability of the formulated suspension.

Entrapment efficiency

The EE study is useful to evaluate the percentage of drugs present in the phospholipids layer in the ultra-flexible formulation. The EE of the DUFLNS was found to be 84.09% ± 0.4%. The drug loading for the DUFLNS was found to be 8.7% ± 0.5% and was considered to be effective in showing pharmacokinetic and therapeutic efficacy in nanosuspensions.

FTIR study

The interactions were determined using FTIR spectroscopy that is likely to occur between diosmin and other constituents of the ultra-flexible liposomes. By comparing the FTIR spectra, the changes in specific diosmin molecule regions were observed due to the interaction with phospholipids. In the optimized formulation, the change from 3,500 to 3,300 cm^{-1} in the stretching frequency of the phenolic O–H of diosmin was examined. The optimized formulation retained all the peaks that were observed in the excipients [36].

DSC study

It is a well-established method to investigate the thermal behavior approach to explain the complex shape of solid-state matter. DSC thermal analysis was studied for soya lecithin, cholesterol, sodium deoxycholate, diosmin, and DUFLNS. The pure diosmin displayed a broad endothermic peak at 298.69°C, analogous to its melting point. Generally, the crystalline nature of the phytoconstituents due to their improper size distribution in crystallinity and also by the loss of water molecules shows a broadening of melting point [37]. Soya lecithin displayed a peak at 183.85°C, and cholesterol and sodium deoxycholate showed an endothermal peak at 139.35°C and 208.73°C, respectively. Furthermore, DUFLNS thermal analysis Figure 3 displayed a wide endothermal peak at 124.76°C.

Transmission electron microscopy

The TEM image of the DUFLNS is shown in Figure 4. TEM studies exhibited a good morphological character related to their size as well as shape. Images revealed that the ultra-

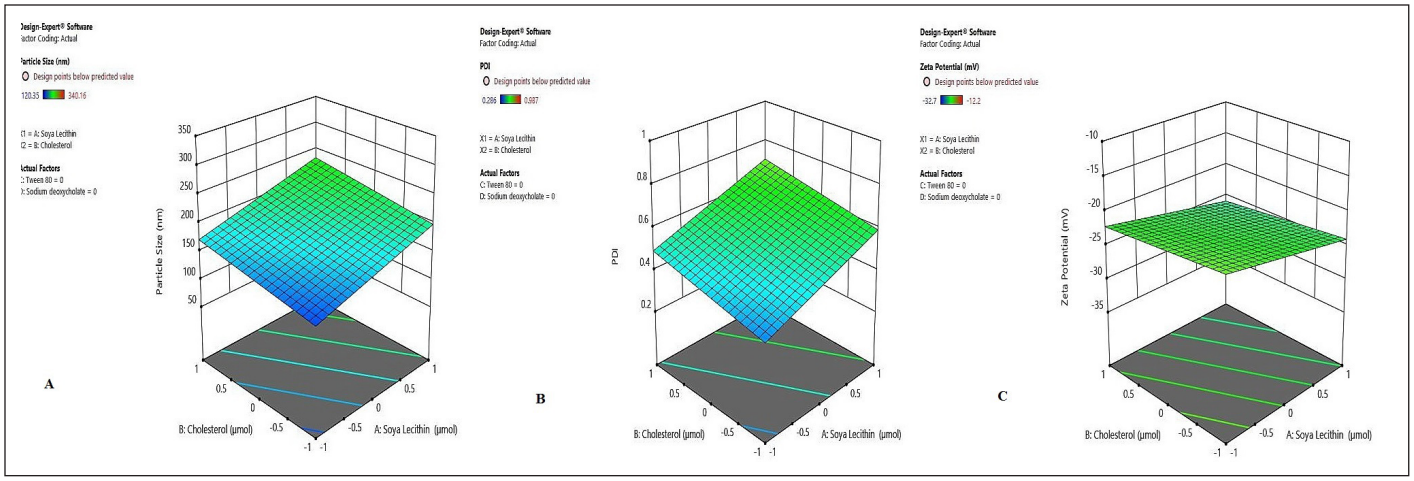

Figure 2. Influence of independent variables. (A) Particle size (nm). (B) PDI. (C) Zeta potential (mV).

Table 3. Selected solutions and the % error between the predicted and the observed values.

Factors				Responses		
A	**B**	**C**	**D**	**PS**	**PDI**	**ZP**
Predicted						
–0.776	–1.000	0.999	–1.000	144.567	0.397	–24.000
Observed						
		98.60			0.368	–24.5
Relative error (%)				31.79	7.30	2.08

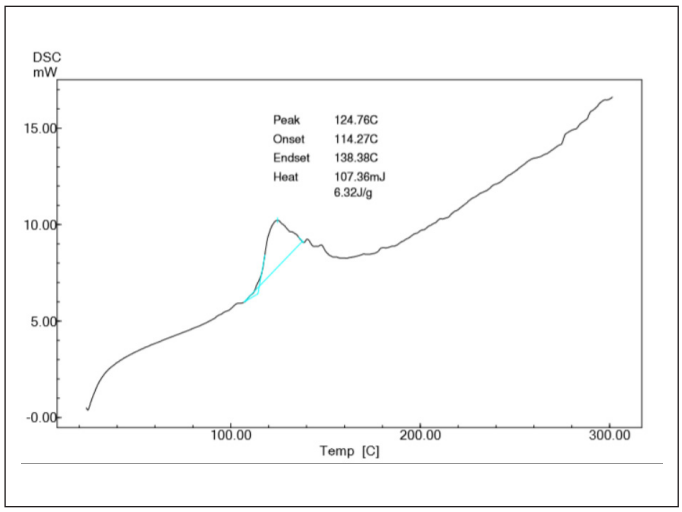

Figure 3. DSC thermogram of DUFLNS.

flexible liposomes were smooth, rounded edges with sub-micron distribution and nanosized size range below 200 nm.

AFM

The AFM image of the DUFLNS is depicted in Figure 5. The AFM scan revealed distinct, well-formed vesicles. When the sample was mounted on a glass slide, it formed vesicular nanostructures with no evidence of aggregation or decomposition owing to its electrostatic repulsive stability. This was determined by ZP measurements, indicating improved suspension stability [38].

Turbidity measurement

The number of vesicles that could be present in the suspension was directly determined by the turbidity value of DUFLNS, which was found to be 25.6 ± 0.004 NTU. Therefore, turbidity is proportional to the amount of surfactant in the colloidal suspension [39].

Evaluation of DUFLGS and DCGS

Measurement of pH

The pH measurement is an essential parameter for topical formulations. If the pH varies from the normal skin pH condition, it may irritate the skin. The pH of DUFLGS and DCGS was found to be 5.13 and 5.46, respectively. Both gel's pH levels were determined to be between 4 and 6, which is much more in line with the skin's pH [40].

Viscosity study

The viscosity of preparation is an important rheological characteristic that affects its physical as well as mechanical properties, such as consistency and spreadability [41]. The viscosity of the DUFLGS and DCGS was determined at different speeds of 5, 10, 20, 50, and 100 rpm using a

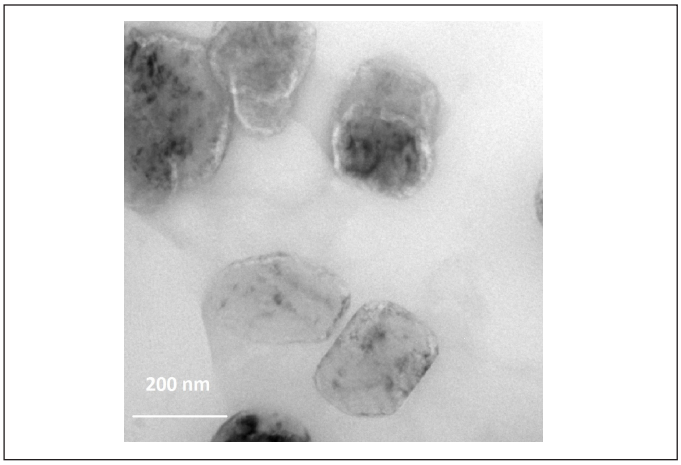

Figure 4. TEM of DUFLNS.

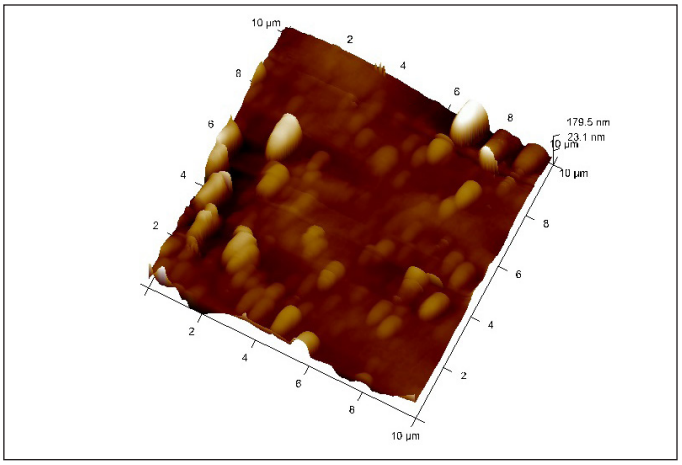

Figure 5. AFM of DUFLNS.

Brookfield viscometer having Spindle No. F96. The viscosity of DUFLGS was found to be in the range of 59–722 cps, whereas DCGS was found to be 57–1,084 cps.

Spreadability

The spreadability of the gel is crucial in the application; if it is poor, the drug's residence time on the skin is hampered, resulting in low bioavailability. The ability to spread DUFLGS was found to be 15.45 g/cm/second, whereas DCGS was found to be 16.12 g/cm/second. The experimental process indicates that the shorter it takes to separate the two slides, the better the spreadability nature of the formulated gel [40].

Drug content

The drug content uniformity for a semi-solid preparation is essential for confirming the homogeneity of the drug dispersed throughout the formulation. The drug content of DUFLGS was found to be 85.33% ± 12%, whereas DCGS was found to be 84.76% ± 11% ($n = 3$). The analysis of the drug concentration revealed that the drug was evenly dispersed all across the gel [42].

Degree of deformability

A distinctive property associated with ultra-flexible vesicles is their deformability, rendering the carrier a possible system for the delivery of topical medications [43]. The deformability of DUFLGS was found to be 95.5 ± 0.14 suggesting that the deformable vesicles regained their size after extrusion whereas the deformability of DCGS was found to be 10.60 ± 0.45, indicating DCGS are quite rigid ($n = 3$) [44].

In vitro skin permeation, deposition study, and release study

The investigations on *in vitro* skin penetration were carried out on goat abdominal skin as it bears a resemblance to the human epithelium and also exhibits a similar absorption pattern. Based on the results, the plot of time (hour) against the cumulative percentage drug permeation rate (µg cm^2) was reported ($n = 3$). At the end of 12 hours, it was found that the cumulative amount of drug permeation of DUFLNS was higher than DUFLGS and DCGS. The cumulative amount permeation of DUFLNS was found to be 900 ± 0.14 µg cm^2, whereas DUFLGS had 795 ± 0.18 µg cm^2 and DCGS had 500 ± 13 µg cm^2 in 12 hours. The result clearly shows the impact of deformability in DUFLNS and DUFLGS; however, DUFLGS was better because of better residence time at the site [43]. The results of DUFLNS, DUFLGS, and DCGS showed skin retention values of 55.5% ± 13%, 83.44% ± 12%, and 66.39% ± 14%, respectively ($n = 3$). The outcomes of the *in vitro* release study demonstrated that the drug release of DUFLGS was found to be 85.14% ± 12% and in a sustained manner, whereas DUFLNS and DCGS had burst and quick release of 62.37% ± 14% and 44.84% ± 12%, respectively, in 12 hours ($n = 3$) (Fig. 6B). In the conventional gel of diosmin, initially, there was a burst effect during the first 6 hours most likely due to the free drug present in the formulation.

In vitro drug release kinetics

The drug release kinetics was examined using four models, i.e., zero, first order, Higuchi, and Korsmeyer-peppas model in the ability to forecast the drug release kinetic mechanism [45]. The slope of appropriate plots was used to estimate the release kinetics, and the regression analysis (R^2) was calculated. The *in vitro* drug release of DUFLNS, DUFLGS, and DCGS was best described by the Higuchi model as the plots displayed the maximum linearity. According to the Higuchi model, the release from the optimized formulation followed a diffusion-controlled mechanism. The values of the regression coefficient (R^2), i.e., 0.992 for DUFLNS, 0.997 for DUFLGS, and 0.984 for DCGS, prove that the release of the drug was essentially independent of the drug's concentration. The value of "n" was found to be –0.144 for DUFLNS, –0.19 for DUFLGS, and 0.984 for DCGS (Table 4). The value of "n" indicates the release mechanism from the formulation and helps understand the drug release kinetics. A value of "n" between 0.45 and 0.89 suggests a Fickian (case I) release mechanism, while a value between 0.89 and 1.0 indicates an anomalous (non-Fickian) transport. If the value of "n" is 0.45, it suggests a case II transport mechanism. Hence, the optimized formulation follows the case II transport mechanism [35].

Table 4. Mathematical model of drug release.

Formulation	Model	R^2	*K*	*n*
DUFLNS	Zero order	0.929	–0.093	-
	First order	0.956	–0.043	-
	Higuchi	0.992	2.051	-
	Korsemeyer-Peppas	0.968	0.672	–0.144
DUFLGS	Zero order	0.977	–0.114	-
	First order	0.952	–0.049	-
	Higuchi	0.997	2.581	-
	Korsemeyer-Peppas	0.988	0.727	–0.19
DCGS	Zero order	0.052	0.031	-
	First order	0.006	–0.004	-
	Higuchi	0.984	4.447	-
	Korsemeyer-Peppas	0.113	–0.506	2.138

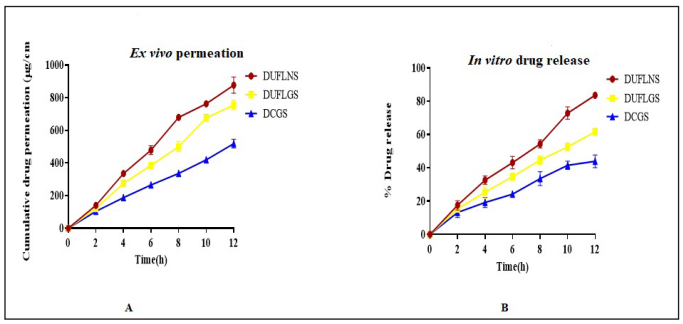

Figure 6. (A) *Ex vivo* permeation study. (B) *In vitro* drug release study of DUFLNS, DUFGS, DCGS.

DISCUSSION

In the present investigation, a lipid nanosuspension was included in a carbopol gel base to develop an ultra-flexible lipid gel system. Jelly bases tend to be used in topical applications since the formulation needs to stay on the skin for an extended period. The anti-inflammatory properties of the drug diosmin were showcased based on the docking score, diosmin is believed to show significant inhibition of proactive cytokines such as TNF-α and IL-6 by interacting and high affinity binding with NIK which is responsible for inflammation and pain in varicose vein condition [46]. Hence, the docking study demonstrates the drug's therapeutic efficiency in the treatment of varicose veins. Designing an optimal formulation was made possible by DoE studies that took account of a central composite model for all three variables of PS, PDI, and ZP. The ultra-flexible smaller PS of less than 200 nm is responsible for the deeper penetration through skin follicles and drugs retain for a longer time into a follicular reservoir. The better EE of the drug could be due to the higher affinity of the drug miscibility in stable phospholipid layers [47]. In the FTIR study, the changes in the formulation peak could result from weak intermolecular interactions formed during the development of DUFLNS. The DSC thermogram of the drug and other excipients for the formulations denotes the change from a gel to a liquid-crystalline state in terms of physical state, and the carbon group in the phospholipid may have possibly led to another different arrangement in atoms or crystal changes. In the formulation of DUFLNS, the shifting of the peak toward lower temperatures may be attributed to the formulation's improved solubility and decreased hydrophobicity due to decreased crystallinity of the drug. This may be due to the drug-phospholipid interaction that is created when diosmin combines with the long hydrocarbon chain tails of phospholipid molecules [48]. The surface morphology through TEM and AFM of the DUFLNS was analyzed and interpreted, due to the lesser the particles, which can cross the subcutaneous layer of the skin without any external influence and reach the target through the shunt pathway possessed by sweat glands. The DUFLGS formulation met scrutiny in terms of pH, viscosity, and spreadability, these are the essential characteristics of any semi-solid preparation for effective drug delivery. The incorporation of the surfactant sodium deoxycholate contributes to the degree of deformability of DUFLGS; it facilitates the squeezing of the lipid bilayers without breaking or losing the drug, thus enabling DUFLGS to penetrate the stratum corneum by altering its intercellular lipids and increasing fluidity. The result of the skin retention study indicates a significant amount of gel retained on the skin membrane due to the presence of an edge activator. Therefore, it acts as a depot and is released in a controlled manner [49]. The results of the *in vitro* release studies demonstrated the importance of the emulsifier and edge activator as well as improved drug partitioning in the formulations (DUFLGS and DUFLNS). The sustained delivery of the DUFLGS is due to the adaptability of the ultra-flexible liposomes, thereby the penetration is enhanced [50].

Therefore, the study offers information on the formulation characteristics of topical, second-generation liposomes in the form of an ultra-flexible lipid gel. The outcome demonstrated greater diosmin permeability with extended release from the gel system, which can be effectively employed for varicose vein treatment.

CONCLUSION

The current study's objectives were to develop and assess an ultra-flexible diosmin-loaded topical gel to treat

varicose veins. The study serves as the first topical application to treat varicose veins wherein an *in-silico* analysis that verifies the drug diosmin's potential interaction with NF-κB initiating kinase receptor binding demonstrated the drug's potential. The *in vitro* results were quite encouraging for permeation and the release of the disomin from ultra-flexible lipid base gel and *in vivo* study can be acted upon to justify further the novelty of the preparation. Due to several advantages associated with the topical route, an in-depth study has been conducted during the last few years on the advancement of topical drug delivery. For the treatment of varicose veins, either surgical procedures or parenteral drug delivery is employed. Hence, to minimize pain and improve patient compliance, the ultra-flexible gel of diosmin was successfully developed to treat varicose veins.

ACKNOWLEDGMENT

The authors are highly thankful to NGSM Institute of Pharmaceutical Sciences, Mangalore, and Manipal College of Pharmaceutical Sciences, Manipal, for providing the resources for the conduction of this research work.

AUTHOR CONTRIBUTIONS

All authors made substantial contributions to conception and design, acquisition of data, or analysis and interpretation of data; took part in drafting the article or revising it critically for important intellectual content; agreed to submit to the current journal; gave final approval of the version to be published; and agree to be accountable for all aspects of the work. All the authors are eligible to be an author as per the International Committee of Medical Journal Editors (ICMJE) requirements/guidelines.

FINANCIAL SUPPORT

There is no funding to report.

CONFLICT OF INTEREST

The authors report no financial or any other conflicts of interest in this work.

ETHICAL APPROVALS

This study does not involve experiments on animals or human subjects.

DATA AVAILABILITY

All data generated and analyzed are included in this research article.

PUBLISHER'S NOTE

This journal remains neutral with regard to jurisdictional claims in published institutional affiliation.

REFERENCES

1. Varicose veins: overview. In: InformedHealth.org [Internet]. Institute for Quality and Efficiency in Health Care (IQWiG); 2019 [cited 2023 Aug 5]. Available from: https://www.ncbi.nlm.nih.gov/books/NBK279247/
2. Jacobs BN, Andraska EA, Obi AT, Wakefield TW. Pathophysiology of varicose veins. J Vasc Surg Venous Lymphat Disord. 2017;5(3):460–7. doi: https://doi.org/10.1016/j.jvsv.2016.12.014
3. Akoijam M, Sangita A, Malar M, Kodi SM. Prevention of varicose veins. J Nurs Sci Pract. 2014;4(1):23–9.
4. Parihar S, Sarswati, Chattarpal, Sharma D. A brief review on herbs used in the treatment of varicose veins. J Drug Deliv Ther. 2022;12(1):158–62. doi: https://doi.org/10.22270/jddt.v12i1.5161
5. Silambarasan T, Raja B. Diosmin, a bioflavonoid reverses alterations in blood pressure, nitric oxide, lipid peroxides and antioxidant status in DOCA-salt induced hypertensive rats. Eur J Pharmacol. 2012;679(1–3):81–9. doi: https://doi.org/10.1016/j.ejphar.2011.12.040
6. Feldo M, Woźniak M, Wójciak-Kosior M, Sowa I, Kot-Waśik A, Aszyk J, *et al*. Influence of diosmin treatment on the level of oxidative stress markers in patients with chronic venous insufficiency. Oxid Med Cell Longev. 2018;2018:2561705. doi: https://doi.org/10.1155/2018/2561705
7. Imam F, Al-Harbi NO, Al-Harbi MM, Ansari MA, Zoheir KMA, Iqbal M, *et al*. Diosmin downregulates the expression of T cell receptors, pro-inflammatory cytokines and NF-κB activation against LPS-induced acute lung injury in mice. Pharmacol Res. 2015;102:1–11. doi: https://doi.org/10.1016/j.phrs.2015.09.001
8. Rai S, Pandey V, Rai G. Transfersomes as versatile and flexible nano-vesicular carriers in skin cancer therapy: the state of the art. Nano Rev Exp. 2017;8(1):1325708. doi: https://doi.org/10.1080/20022727.2017.1325708
9. Gupta R, Kumar A. Transfersomes: the ultra-deformable carrier system for non-invasive delivery of drug. Curr Drug Deliv. 2021;18(4):408–20. doi: https://doi.org/10.2174/1567201817666200804105416
10. de Leon-Boenig G, Bowman KK, Feng JA, Crawford T, Everett C, Franke Y, *et al*. The crystal structure of the catalytic domain of the NF-κB inducing kinase reveals a narrow but flexible active site. Structure. 2012;20(10):1704–14. doi: https://doi.org/10.1016/j.str.2012.07.013
11. Ali A, Abdellattif MH, Ali A, AbuAli O, Shahbaaz M, Ahsan MJ, *et al*. Computational approaches for the design of novel anticancer compounds based on Pyrazolo[3,4-d]pyrimidine derivatives as TRAP1 inhibitor. Molecules. 2021;26(19):5932. doi: https://doi.org/10.3390/molecules26195932
12. Malakar J, Sen SO, Nayak AK, Sen KK. Formulation, optimization and evaluation of transferosomal gel for transdermal insulin delivery. Saudi Pharm J. 2012;20(4):355–63. doi: https://doi.org/10.1016/j.jsps.2012.02.001
13. Vasanth S, Dubey A, Ravi GS, Lewis SA, Ghate VM, El-Zahaby SA, *et al*. Development and investigation of Vitamin C-enriched adapalene-loaded transfersome gel: a collegial approach for the treatment of acne vulgaris. AAPS PharmSciTech. 2020;21(2):61. doi: https://doi.org/10.1208/s12249-019-1518-5
14. Jangdey MS, Gupta A, Saraf S, Saraf S. Development and optimization of apigenin-loaded transfersomal system for skin cancer delivery: *in vitro* evaluation. Artif Cells Nanomed Biotechnol. 2017;45(7):1452–62. doi: https://doi.org/10.1080/21691401.2016.1247850
15. Thakur N, Jain P, Jain V. Formulation development and evaluation of transferosomal gel. J Drug Deliv Ther. 2018;8:168–77. doi: https://doi.org/10.22270/jddt.v8i5.1826
16. Qin T, Dai Z, Xu X, Zhang Z, You X, Sun H, *et al*. Nanosuspension as an efficient carrier for improved ocular permeation of voriconazole. Curr Pharm Biotechnol. 2021;22(2):245–53. doi: https://doi.org/10.2174/1389201021999200820154918
17. Shilakari Asthana G, Sharma PK, Asthana A. *In vitro* and *in vivo* evaluation of niosomal formulation for controlled delivery of clarithromycin. Scientifica. 2016;2016:6492953. doi: https://doi.org/10.1155/2016/6492953
18. Srilatha D, Nasare M, Nagasandhya B, Prasad V, Diwan P. Development and validation of UV spectrophotometric method for simultaneous estimation of hesperidin and diosmin in the

pharmaceutical dosage form. Int Sch Res Notices. 2013;2013:534830. doi: https://doi.org/10.1155/2013/534830
19. Kassem MA, Aboul-Einien MH, El Taweel MM. Dry gel containing optimized felodipine-loaded transferosomes: a promising transdermal delivery system to enhance drug bioavailability. AAPS PharmSciTech. 2018;19(5):2155–2173. doi: https://doi.org/10.1208/s12249-018-1020-5
20. Agiba AM, Nasr M, Abdel-Hamid S, Eldin AB, Geneidi AS. Enhancing the intestinal permeation of the chondroprotective nutraceuticals glucosamine sulphate and chondroitin sulphate using conventional and modified liposomes. Curr Drug Deliv. 2018;15(6):907–16. doi: https://doi.org/10.2174/1567201815666180123100148
21. Telange DR, Patil AT, Pethe AM, Fegade H, Anand S, Dave VS. Formulation and characterization of an apigenin-phospholipid phytosome (APLC) for improved solubility, *in vivo* bioavailability, and antioxidant potential. Eur J Pharm Sci. 2017;108:36–49. doi: https://doi.org/10.1016/j.ejps.2016.12.009
22. Ravi GS, Charyulu RN, Dubey A, Prabhu P, Hebbar S, Mathias AC. Nano-lipid complex of rutin: development, characterisation and *in vivo* investigation of hepatoprotective, antioxidant activity and bioavailability study in rats. AAPS PharmSciTech. 2018;19(8):3631–49. doi: https://doi.org/10.1208/s12249-018-1195-9
23. Robson AL, Dastoor PC, Flynn J, Palmer W, Martin A, Smith DW, *et al*. Advantages and limitations of current imaging techniques for characterizing liposome morphology. Front Pharmacol. 2018;9:80. doi: https://www.frontiersin.org/articles/10.3389/fphar.2018.00080
24. Lee H, Bang JB, Na YG, Lee JY, Cho CW, Baek JS, *et al*. Development and evaluation of tannic acid-coated nanosuspension for enhancing oral bioavailability of curcumin. Pharmaceutics. 2021;13(9):1460. doi: https://doi.org/10.3390/pharmaceutics13091460
25. Ashoori Y, Mohkam M, Heidari R, Abootalebi SN, Mousavi SM, Hashemi SA, *et al*. Development and *in vivo* characterization of probiotic lysate-treated chitosan nanogel as a novel diocompatible formulation for wound healing. BioMed Res Int. 2020;2020:e8868618. doi: https://doi.org/10.1155/2020/8868618
26. Alam MdS, Algahtani MS, Ahmad J, Kohli K, Shafiq-un-Nabi S, Warsi MH, *et al*. Formulation design and evaluation of aceclofenac nanogel for topical application. Ther Deliv. 2020;11(12):767–78. doi: https://doi.org/10.4155/tde-2020-0076
27. Elkomy MH, El Menshawe SF, Eid HM, Ali AMA. Development of a nanogel formulation for transdermal delivery of tenoxicam: a pharmacokinetic–pharmacodynamic modeling approach for quantitative prediction of skin absorption. Drug Dev Ind Pharm. 2017;43(4):531–44. doi: https://doi.org/10.1080/03639045.2016.1268153
28. Sood R, Chopra DS. Optimization of reaction conditions to fabricate Ocimum sanctum synthesized silver nanoparticles and its application to nano-gel systems for burn wounds. Master Sci Eng C Mater Biol Appl. 2018;92:575–89. doi: https://doi.org/10.1016/j.msec.2018.06.070
29. Luckanagul JA, Pitakchatwong C, Ratnatilaka Na Bhuket P, Muangnoi C, Rojsitthisak P, Chirachanchai S, *et al*. Chitosan-based polymer hybrids for thermo-responsive nanogel delivery of curcumin. Carbohydr Polym. 2018;181:1119–27. doi: https://doi.org/10.1016/j.carbpol.2017.11.027
30. Panonnummal R, Jayakumar R, Sabitha M. Comparative anti-psoriatic efficacy studies of clobetasol loaded chitin nanogel and marketed cream. Eur J Pharm Sci. 2017;96:193–206. doi: https://doi.org/10.1016/j.ejps.2016.09.007
30. Peralta MF, Guzmán ML, Pérez AP, Apezteguia GA, Fórmica ML, Romero EL, *et al.* Liposomes can both enhance or reduce drugs penetration through the skin. Sci Rep. 2018;8(1):13253. doi: https://doi.org/10.1038/s41598-018-31693-y
31. Khurana S, Bedi PMS, Jain NK. Preparation and evaluation of solid lipid nanoparticles based nanogel for dermal delivery of meloxicam. Chem Phys Lipids. 2013;175–176:65–72. doi: https://doi.org/10.1016/j.chemphyslip.2013.07.010
32. Gondkar SB, Patil NR, Saudagar RB. Formulation development and characterization of etodolac loaded transethosomes for transdermal delivery. Res J Pharm Technol. 2017;10(9):3049–57. doi: https://doi.org/10.5958/0974-360X.2017.00541.8
33. Desu PK, Karmakar B, Kondi V, Tiwari ON, Halder G. Optimizing formulation of green tea extract-loaded chitosan nanogel. Biomass Conv Bioref. 2022. doi: https://doi.org/10.1007/s13399-022-02453-w
34. Higuchi T. Rate of release of medicaments from ointment bases containing drugs in suspension. J Pharm Sci. 1961;50:874–5. doi: https://doi.org/10.1002/jps.2600501018
36. Atta AM, El-Azabawy OE, Ismail HS, Hegazy MA. Novel dispersed magnetite core–shell nanogel polymers as corrosion inhibitors for carbon steel in acidic medium. Corros Sci. 2011;53(5):1680–9. doi: https://doi.org/10.1016/j.corsci.2011.01.019
37. Gill P, Moghadam TT, Ranjbar B. Differential scanning calorimetry techniques: applications in biology and nanoscience. J Biomol Tech. 2010;21(4):167–93.
38. Bahri A, Martin M, Gergely C, Marchesseau S, Chevalier-Lucia D. Topographical and nanomechanical characterization of casein nanogel particles using atomic force microscopy. Food Hydrocoll. 2018;83:53–60. doi: https://doi.org/10.1016/j.foodhyd.2018.03.029
39. Brijitta J, Tata BVR, Kaliyappan T. Phase behavior of poly(N-isopropylacrylamide) nanogel dispersions: temperature dependent particle size and interactions. J Nanosci Nanotechnol. 2009;9(9):5323–8. doi: https://doi.org/10.1166/jnn.2009.1144
40. Hayashi H, Iijima M, Kataoka K, Nagasaki Y. pH-sensitive nanogel possessing reactive PEG tethered chains on the surface. Macromolecules. 2004;37(14):5389–96. doi: https://doi.org/10.1021/ma049199g
41. Kumar S, Singh KK, Rao R. Enhanced anti-psoriatic efficacy and regulation of oxidative stress of a novel topical babchi oil (*Psoralea corylifolia*) cyclodextrin-based nanogel in a mouse tail model. J Microencapsul. 2019;36(2):140–55. doi: https://doi.org/10.1080/02652048.2019.1612475
42. Eckmann DM, Composto RJ, Tsourkas A, Muzykantov VR. Nanogel carrier design for targeted drug delivery. J Mater Chem B Master Biol Med. 2014;2(46):8085–97. doi: https://doi.org/10.1039/C4TB01141D
43. Divya G, Panonnummal R, Gupta S, Jayakumar R, Sabitha M. Acitretin and aloe-emodin loaded chitin nanogel for the treatment of psoriasis. Eur J Pharm Biopharm. 2016;107:97–109. doi: https://doi.org/10.1016/j.ejpb.2016.06.019
44. Zhang ZJ, Osmałek T, Michniak-Kohn B. Deformable liposomal hydrogel for dermal and transdermal delivery of meloxicam. Int J Nanomed. 2020;15:9319–35. doi: https://doi.org/10.2147/IJN.S274954
45. Ashfaq A, An JC, Ulański P, Al-Sheikhly M. On the mechanism and kinetics of synthesizing polymer nanogels by ionizing radiation-induced intramolecular crosslinking of macromolecules. Pharmaceutics. 2021;13(11):1765. doi: https://doi.org/10.3390/pharmaceutics13111765
46. Feldo M, Wójciak-Kosior M, Sowa I, Kocki J, Bogucki J, Zubilewicz T, *et al*. Effect of diosmin administration in patients with chronic venous disorders on selected factors affecting angiogenesis. Molecules. 2019;24(18):3316. doi: https://doi.org/10.3390/molecules24183316
47. Maiti K, Mukherjee K, Gantait A, Saha BP, Mukherjee PK. Curcumin-phospholipid complex: preparation, therapeutic evaluation and pharmacokinetic study in rats. Int J Pharm. 2007;330(1–2):155–63. doi: https://doi.org/10.1016/j.ijpharm.2006.09.025
48. Aminu N, Chan SY, Yam MF, Toh SM. A dual-action chitosan-based nanogel system of triclosan and flurbiprofen for localised treatment

of periodontitis. Int J Pharm. 2019;570:118659. doi: https://doi.org/10.1016/j.ijpharm.2019.118659
49. Lei M, Zhang W, Yi C, Yan L, Tian Y. Zwitterionic nanogels with temperature sensitivity and redox-degradability for controlled drug release. Colloids Surf B Biointerfaces. 2021;206:111959. doi: https://doi.org/10.1016/j.colsurfb.2021.111959
50. Wu HQ, Wang CC. Biodegradable smart nanogels: a new platform for targeting drug delivery and biomedical diagnostics. Langmuir. 2016;32(25):6211–25. doi: https://doi.org/10.1021/acs.langmuir.6b00842

How to cite this article:
Dubey A, Shetty A, Shetty CR, Dhas N, Naha A, Bhandary P, Hebbar S. Design and assessment of *in silico* screened diosmin incorporated ultra-flexible topical lipid gel system for the treatment of varicose vein. J Appl Pharm Sci. 2024;14(04):143–154.